UNIVERSITI
MALAYSIA
PERLIS

Correlation between the Calcination and Sintering Temperature on Phase Formation, Microstructure and Dielectric Properties of SrTiO₃ Ceramics

Abdelhalim Elbasset[1,2*], Tajddin. Lamcharfi[1], Farid Abdi[1], Hicham Laribou[3], abdelhak elghandouri[2] and Lamiae mrharrab[2]

[1]LSSC, Department of Electrical Engineering, Faculty of Science and Technology (FST) B.P.2202, University Sidi Mohamed Ben Abdellah, Fes, Morocco
[2]Laboratory of Physics, Theoretical and Applied, FSDM B.P. 179, Fez. Morocco
[3]Laboratory for microstructures and materials mechanics. University of Lorraine, Metz, France

ABSTRACT

The aim of this work is to investigate the effect of calcination temperature (600, 700 and 800°C) and sintering temperature (1000, 1050 and 1100°C) on pure phase formation, microstructure and dielectric properties of perovskite SrTiO₃ (ST) ceramics. The results show that the calcination conditions at 600°C for 6h, are sufficient to obtain this phase. Furthermore, lattice parameter (a) tends to increase with increasing calcinations temperature. The Raman spectroscopy characterization indicates the presence in the calcination spectrum at 600°C of extra-modes located around 113 and 617 cm⁻¹. The optical absorption edge of SrTiO₃ was explored in the temperature from 200 to 1000°C. The results suggest that the band gap energy is increasing with temperature. On the other hand, the results found show that the average grain size of the sintered ST at 1100°C is the order of 12µm which is respectively larger than that at 1000 (~ 3.2µm) and at 1050°C (~ 6.4µm). The dielectric study shows that samples sintered at 1100°C have smaller and stable dielectric losses as a function of frequency.

1. INTRODUCTION

Among ferroelectric ceramics, strontium titanate (SrTiO₃) with perovskite structure is an important electronic material, that has a wide range of industrial and commercial applications, due to their several characteristics, ranging from dielectric properties of superconductivity, via ferroelectricity and semi-conduction. Therefore, strontium titanate is widely used in electronic, mechanical and functional ceramic materials. As a semiconductor material, the band gap of SrTiO₃ is 3.4 eV, under the excitation of ultraviolet light, can produce photogenerated electrons and holes. The reducibility of photogenerated electrons can be used for the hydrolysis of photodecomposition to produce hydrogen, and the oxidation of photogenerated holes can be used for the photodegradation of organic pollutants, which can solve the problems of air pollution. Environment and the energy crisis of the fine. Moreover, strontium titanate (SrTiO₃) is known as low cost materials with high thermal and chemical stability in air [1-3]. According to research reports, the properties of SrTiO₃ are related to its morphology, size, existing external and internal structure. Most scientific research focuses on the properties of SrTiO₃ with higher

---

* Corresponding author: elbasset.abdelhalim@gmail.com/abdelhalim.elbasset@usmba.ac.ma

heat treatment temperatures (700-1200°C) [4, 5, 6], and they are produced by the solid state reaction process [7-15]. This method has a several inconveniences, such as, stoichiometries change, and the secondary phases formation.

Therefore, the type of nanoscale $SrTiO_3$ material is difficult to manufacture by this process, especially as the material conductivity is determined only by controlling the size grain, and the conduction type of the material [16].

To obtain nanoscale materials for a heat treatment with low temperature, the sol-gel method was a very efficient way to prepare nanoscale materials, for important applications as gas or humidity sensors [17, 18-20]. The sol-gel method is one of the simplest techniques to synthesize high quality nano and microstructures, and widely used as a coating method [21-23]. This method provides several advantages over other synthetic routes such as control of material size, texture and surface properties, ease of implementation, high quality and production of large area materials and low cost [24]. This simplicity and flexibility make it very popular in the production of nanoscale powders [25-27], where this work is situated in this context. In the present research, nanometric powders of $SrTiO_3$ are prepared by the sol-gel method to systematically study the influence of the heat treatment, on structural and dielectric properties of $SrTiO_3$.

2. EXPERIMENTAL METHOD

In this study, $SrTiO_3$ were obtained with a sol-gel process by the use of the strontium acetate trihydrate $(Sr(CH_3COO)_2,3H_2O)$; the steps in the preparation the $SrTiO_3$ powders are similar to other previous works [28]. The raw powder obtained after grinding, was calcined at 600, 700, and 800°C (coded as ST6, ST7 and ST8 respectively) for 4 hours and 6 hours in a programmable oven. The reaction progress was followed by an X-ray diffractometer (XRD) with CuKα (λ=1.5405Å) radiation (the diffractometer range, 2θ, was from 10 to 100° with a sweep rate of 4°/min), and by the Raman spectroscopy in the frequency range of 100-1000 cm^{-1}, as in previous work [29-30]. The powder was then pressed into disks of 12mm as diameter and 1mm of thickness under pressure around 450 MPa. The final sintering of the pellets was done at 1000, 1050 and 1100°C for 6h with a heating rate of 3°C. Dielectric characterization was performed as a function of frequency from 1 kHz to 2 MHz. These dielectric measurements were carried out in the temperature range of 25-400°C and under sub weak level of excitement (1v) using an Agilent 4294A precision impedance analyzer (Hewlett-Packard, Palo Alto, CA) as in previous work [30]. The absorption spectrometry was performed and measured by using a Jasco 670 UV spectrometer.

3. RESULTS AND DISCUSSION

Figure 1 shows the XRD patterns for synthesized $SrTiO_3$ samples which calcined at 600, 700 and at 800°C, for 4 and 6 hours, respectively. The results indicate that the reaction's evolution of the ST powder formation depending on the temperature and calcination time. Figure 1 (a) shows the $SrTiO_3$ crystallization in the cubic perovskite phase, with the presence of the secondary phase (TiO_2) at 600°C, and the intensity of the second phase (TiO_2) decreases at 700°C. However, this result showed that the increase in the calcination temperature (at 800°C) lead to the formation of a well crystalline single phase of $SrTiO_3$ without the presence of secondary phase TiO_2. The peaks located at 22.75, 32.39, 39.94, 46.47, 57.77, 67.80 and 77.18° indicate the presence of $SrTiO_3$ phase at 600, 700 and 800°C (JCPDS card no. 84-0444) which are in perfect agreement with others [31]. On the other hand, Figure 1(b) shows the crystallization of ST from 600°C for 6 hours in the perovskite phase without the presence of the secondary phase. In the following, we will use 6 hours as a calcination time to characterize of $SrTiO_3$. Crystallite size was calculated by using the Debye Scherrer equation from the most intense peak (110) [19]. The results are

presented in Figure 2 and in Table 1, which show that the average crystalline size of $SrTiO_3$ ceramics calcined for 6 hours increases from 20.74 to 30.53 nm as the calcination temperature increases from 600 to 700°C respectively. Moreover, the crystallite size decreases to 20.81 nm at 800°C. In addition, the average grains size of $SrTiO_3$ calcined for 4 hours shows an increase with the calcination temperature followed by a decrease. The average size of the grains of the powders calcined at 600°C is of the order of 18.71 nm (Table 1). Grains size grows and reaches an average size of approximately 29.28 nm when the temperature increased to 700°C and subsequently decreased to 19.18 nm at 800°C. Then, we can conclude that the temperature of 700°C would be a critical value for having materials with nanometric size for a heat treatment with a low temperature. The unit cell volume variation as a function of calcination temperature (for 6 hours) is shown in Figure 3. The results show that the unit cell volume increased with the increasing of calcination temperature. The sample calcined at 600°C has a volume of 59.64 $Å^3$ while the volume of the sample calcined at 800 is 59.74 $Å^3$. This observation is also valid for the other compounds calcined for 4 hours. However, this study also shows that the unit cell volume increases with increasing calcination time.
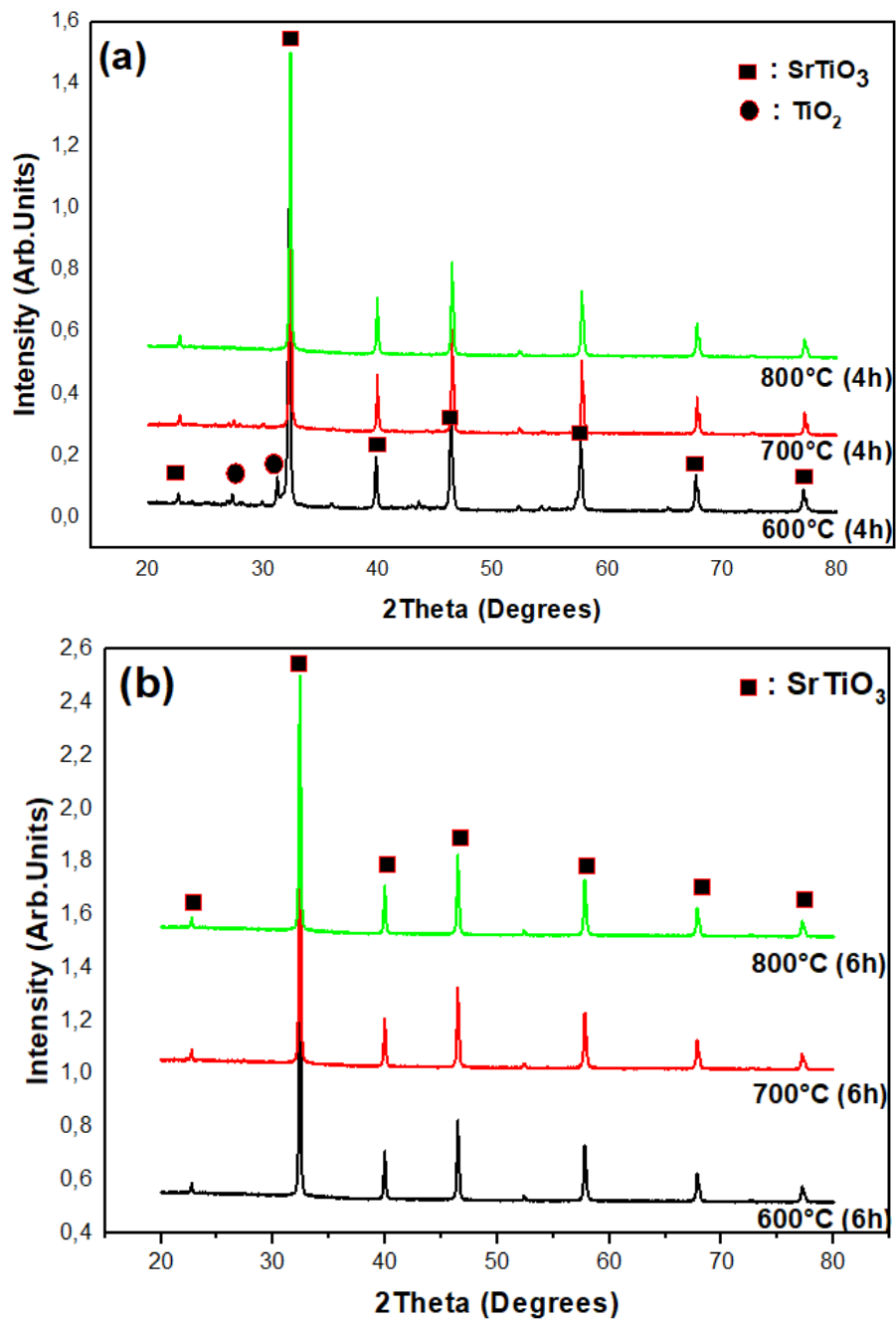
Figure 1. XRD patterns for synthesized SrTiO₃ samples after different calcination temperatures (a) for 4 hours and (b) for 6 hours
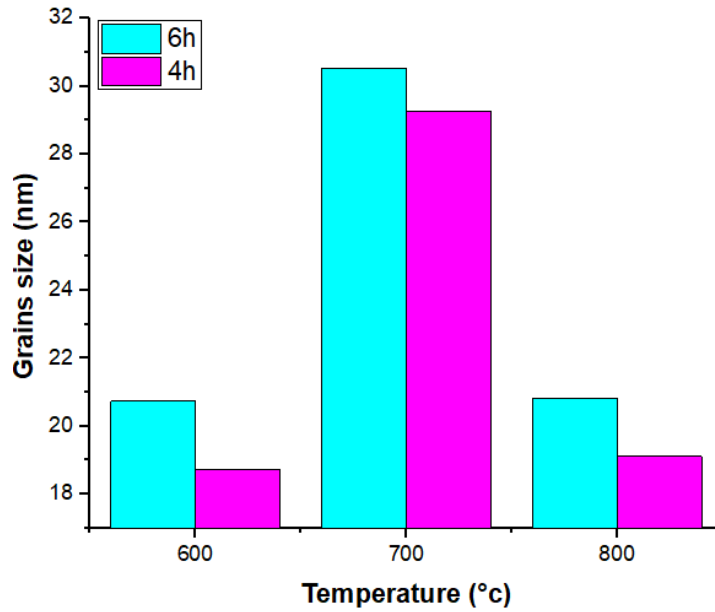
Figure 2. Average grains size of SrTiO$_3$ ceramics calcined at 600,700 and 800°C for 4h and 6h

Table 1 Lattice parameter, a, cell volume, V and average grains size of SrTiO$_3$ ceramics calcined (at 600 to 800°C) for 4 hours and 6 hours

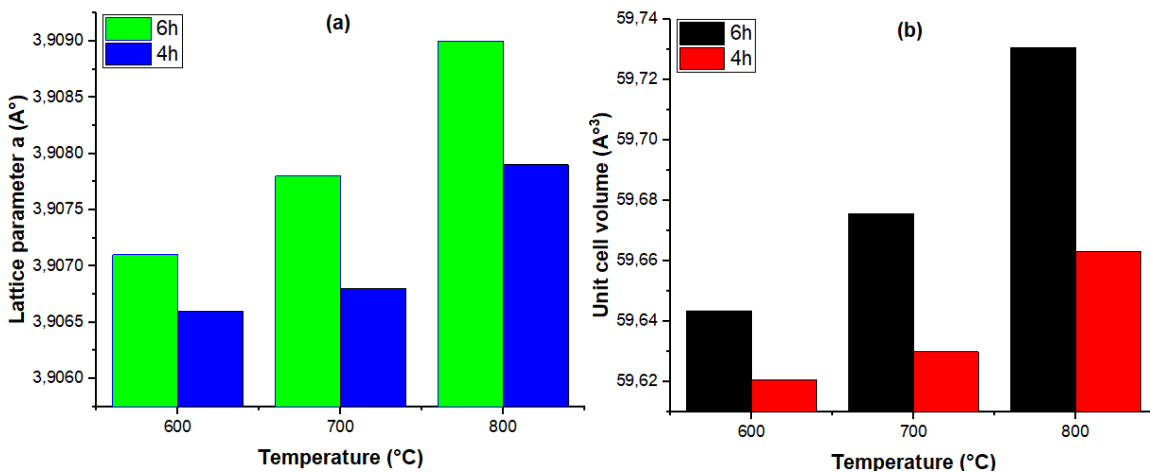| Calcination temperature (°C) for 6h	Mean crystallite size (nm)	a (Å)	V (Å^3)	Calcination temperature (°C) for 4h	Mean crystallite size (nm)	a (Å)	V (Å^3)
600	20.74	3,9071	59,6435	600	18,71	3,9066	59,6207
700	30.53	3,9078	59,6756	700	29,28	3,9068	59,6298
800	20.81	3,9090	59,7306	800	19,12	3,9079	59,6632

Figure 3. Variation of the (a) lattice parameter and (b) the volume of SrTiO$_3$ calcined for 4 hours and 6 hours

Figure 4 shows the evolution of the microstructure of the ST6 sample as a function of the sintering temperature. The microstructure of ST$_6$ sintered at 1100°C shows grain growth and an increase in density and the particle size distribution is more homogeneous compared to the

microstructure than those which sintered at 1000 and 1050°C. Indeed, the average grain size of sintered ST at 1100°C is about 12μm which is larger than that at 1000°C ($\sim$ 3.2μm) and that at 1050°C ($\sim$ 6.4μm). It can be noted that the variation in grain-size increases non-linearly with the sintering temperature as can be seen in Figure 5, thus, the increase in the sintering temperature induces the increase in the grain size which results in the decrease in the grain boundary density, which favors the increase of permittivity [32].
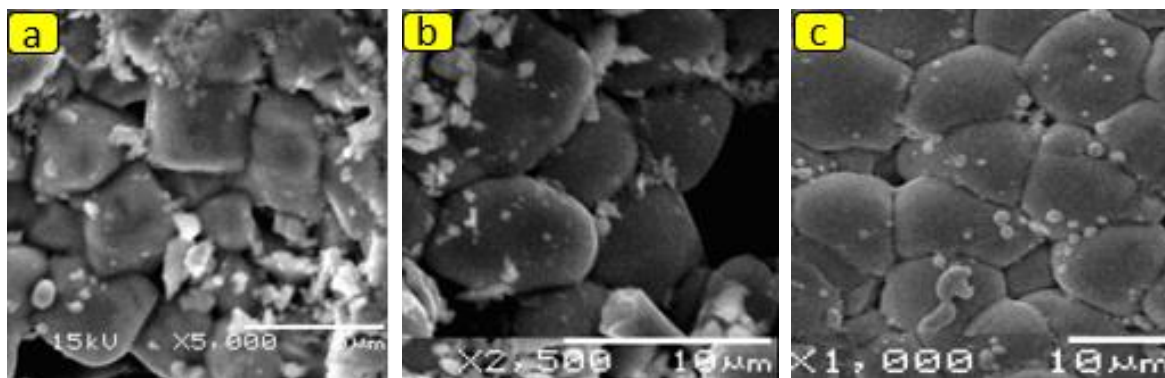

Figure 4. The SEM micrographs of ST6 ceramic calcined at 600°C for 6 hours and sintered at (a) 1000°C (b) 1050°C and (c) 1100°C
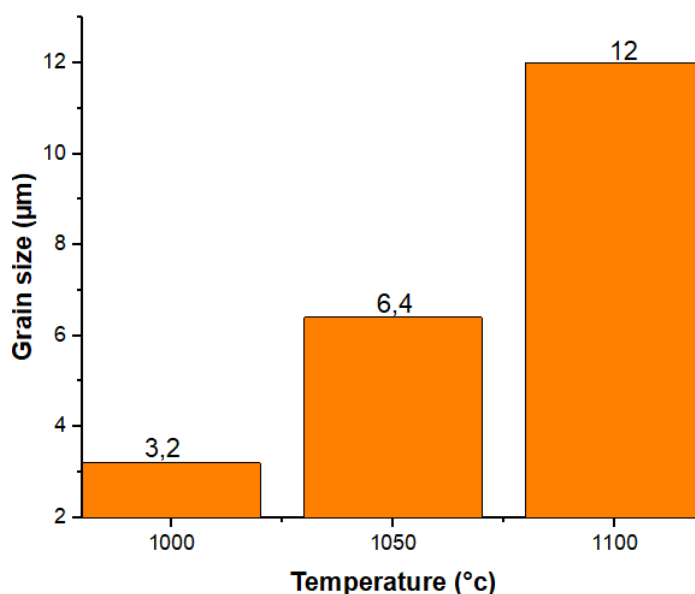

Figure 5. The average grains size of SrTiO$_3$ ceramics calcined at 600°C for 6 hours and sintered at 1000, 1050 and 1100°C

Table 2 Average grains size, and dielectric loss of SrTiO$_3$ ceramics calcined at 600°C (for 6 hours) and sintered at 1000 to 1100°C for 6 hours

Sintering temperature (°C) for 6h	Grain size (μm)	Dielectric loss measured at 400°C (f = 1MHz)
1000	3.20	0.057
1050	6.40	0.023
1100	12.00	0.021

The Raman spectra of the samples which heat treated for six hours are shown in Figure 6 for a wide range of frequency 100-800 cm^{-1}. The results suggest that the Raman bands are well defined

and their intensity varied with the calcination temperature. Our results are consistent with other study [33]. The bands around 246 and 447 cm^{-1} associated with $B_{12}(B_{2g})$ and $R_{25}(B_{1g}+E_g)$ modes, are characteristic of the tetragonal phase. In the tetragonal phase, the $E_{1g} + B_{1g}$ mode of SrTiO$_3$ leads to the emission of a Raman line around 447 cm^{-1}. However, no line at 447cm^{-1} is observed on the other spectra recorded at 600 and 700°C. It suggests that the increase in the temperature of the heat treatment can change the cubic symmetry of SrTiO$_3$. On the other hand, we note the presence of two small peaks located respectively at 173 and 542cm^{-1} associated with TO$_2$ and TO$_4$ modes, especially at low temperature [34]. Their intensities decreased with the calcination temperature and disappeared completely in the case of TO$_4$ at 800°C. These modes are generally attributed to deviations from the cubic structure due to oxygen deficiencies, or the secondary phases with different stoichiometry. Nevertheless, extra-modes at 113 and 617cm^{-1} were indicated on the spectrum recorded at 600°C, but the intensity of that which lies at 113cm^{-1} decreases with the increase of the heat treatment and that of the second band increases with the calcination temperature. Similar to the XRD data, the results of Raman spectroscopy confirms that we have been able to optimize the calcination temperature at 600°C to prepare, by the sol-gel method, the SrTiO$_3$ materials.
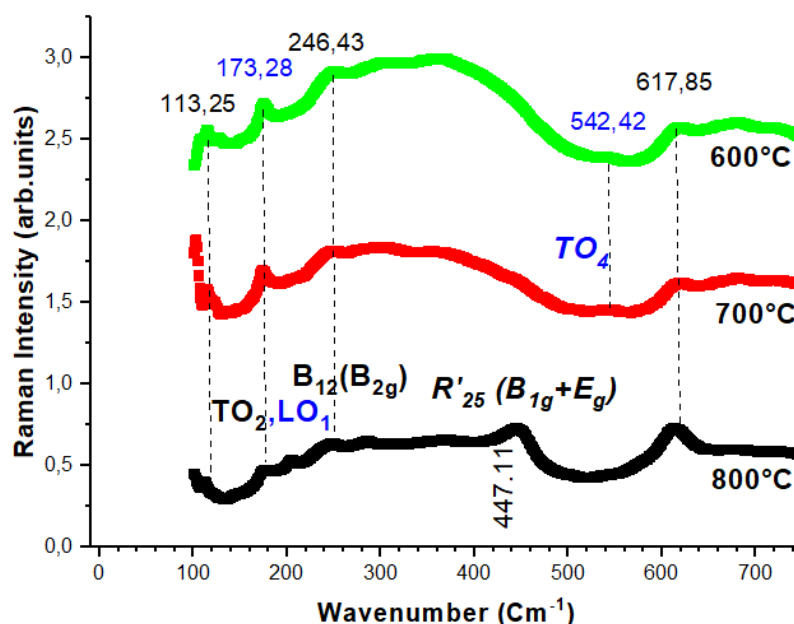

Figure 6. Temperature dependences of the Raman spectra of ST6 samples calcined at 600°C for 6 hours

The optical absorption edge of SrTiO$_3$ was measured at different temperatures from 200 to 1000 °C. Figure 7 shows the band gap of the ST (ST$_6$, ST$_7$ and ST$_8$) materials for various calcinations temperature. The results show that the band gap energy increases with the increase of the heat treatment temperature. The obtained values are closely similar to previous studies [35 -36]. Indeed, at 200°C, the band gap energy increases from 1.10 to 1.83 eV to reach a significant value of 3.32 eV for the three materials S$_6$, S$_7$ and S$_8$ respectively.

These effects have to be considered in high temperature applications of SrTiO$_3$-based devices, as the number of free carriers rises considerably and in bulk crystal growth to avoid growth instabilities. The reduction of the intermediate energy levels within the band gap can be the reason for increase in optical and gap values. These reductions are due to the structure increase or the variation of structural formation into the lattice, as noted in the other work [37-38]. However, other studies [39] have indicated that the band gap may vary due to the change in crystallite size, band gap increases with decreasing grain size. This was not true in our case; therefore, we assume that there are other factors that could affect the band gap energy.
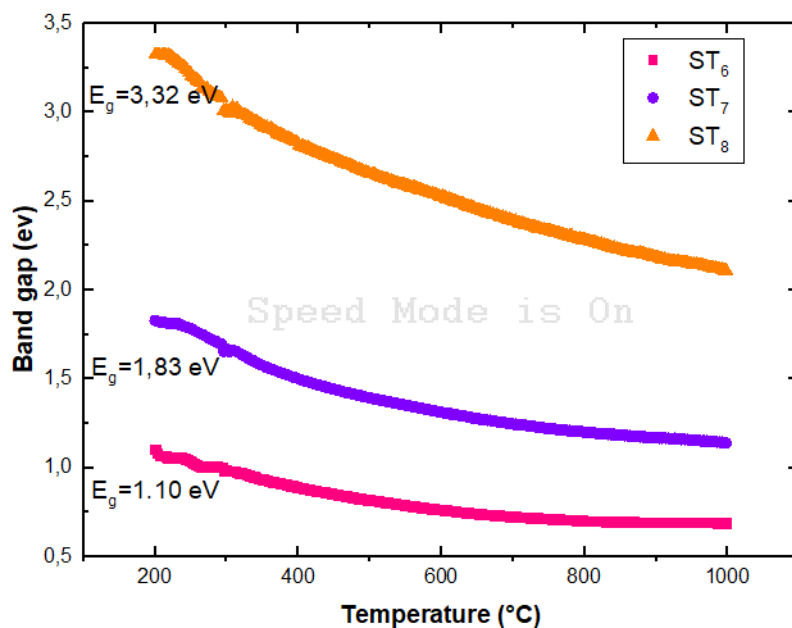
Figure 7. Shows the band gap of the of ST (ST_6, ST_7 and ST_8) materials for various calcinations temperature at 600°C for 6 hours

Figure 8 shows the evolution of the dielectric properties of the ST ceramic as a function of frequency for different measuring. The results obtained show that the dielectric constant of ST_{1000} decreases with increasing frequency above 200 kHz, for different measurement temperatures, except for the samples measured at 200°C, and beyond from this frequency value, it becomes almost constant. Furthermore, we noticed that all the samples sintered at 1050 and 1100°C have a similar dielectric response with frequency. However, we should report that the permittivity decreases with the measurement temperature for sintered sample at 1000°C. Moreover, in Figure 8(c), with sintered sample at 1100°C, the permittivity remains constant for all the measurement temperatures, which is probably explained by the decrease of the density of the grain boundaries where the dielectric permittivity becomes independent of the measured temperature. The results show an interesting stability of the permittivity of sintered ceramics at 110 0°C (especially for f> 100 kHz). On the other hand, the dielectric losses at low frequencies (Figure 8(d), (e) and (f)), decreasing and become almost constant for frequencies above 100 kHz. However, the increase in the measurement temperature induces a decrease in dielectric loss (Figure 8(d)) and shows the reverse trend in Figures 8 (e) and (f). The effect of the sintering temperature on the dielectric properties of ST ceramics is shown schematically in Figure 9.

Although the evolution of dielectric constant as a function of frequency does not change, there is a large difference in dielectric loss for each sample. For example, the dielectric loss measured at 400°C and at the frequency of f = 1 MHz (Table 2), increases with the raise of the sintering temperature, where the values of the samples sintered at 1000, 1050 and 1100°C are 0.057, 0.023 and 0.021 respectively. These values are very small in comparison with other work [31, 40]. Therefore, after all that we have just seen, we can deduce that the samples sintered at 1100°C have a smaller and stable dielectric losses as a function of frequency, which provide a large scale of several applications fields such as surge protection of electronic devices. At last, the dielectric study shows higher responses at lower optimal operating temperatures compared to other work [40].
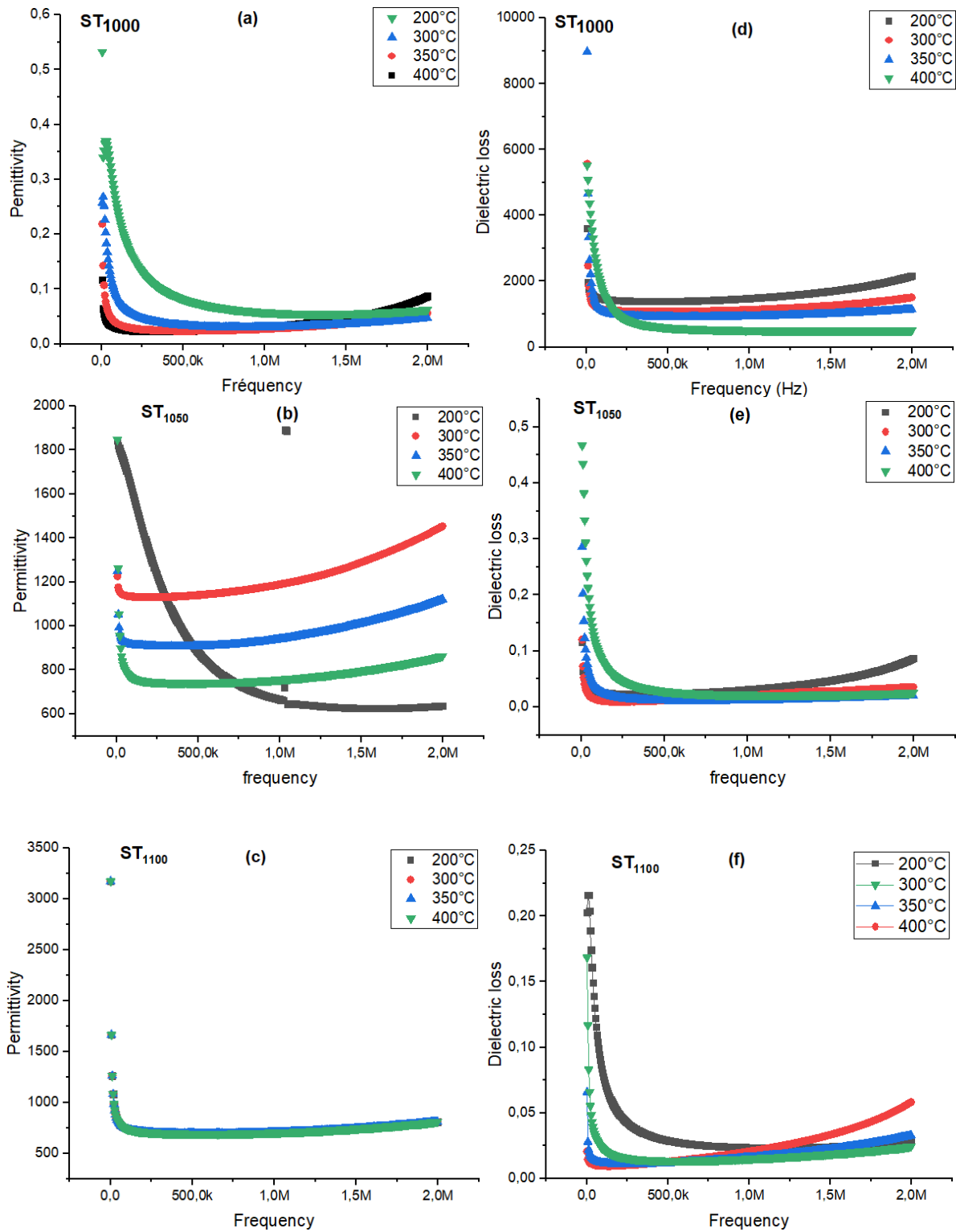
Figure 8. Frequency dependence of permittivity (a, b, c) and dielectric loss (d, e, f) at various temperatures for $SrTiO_3$ ceramics
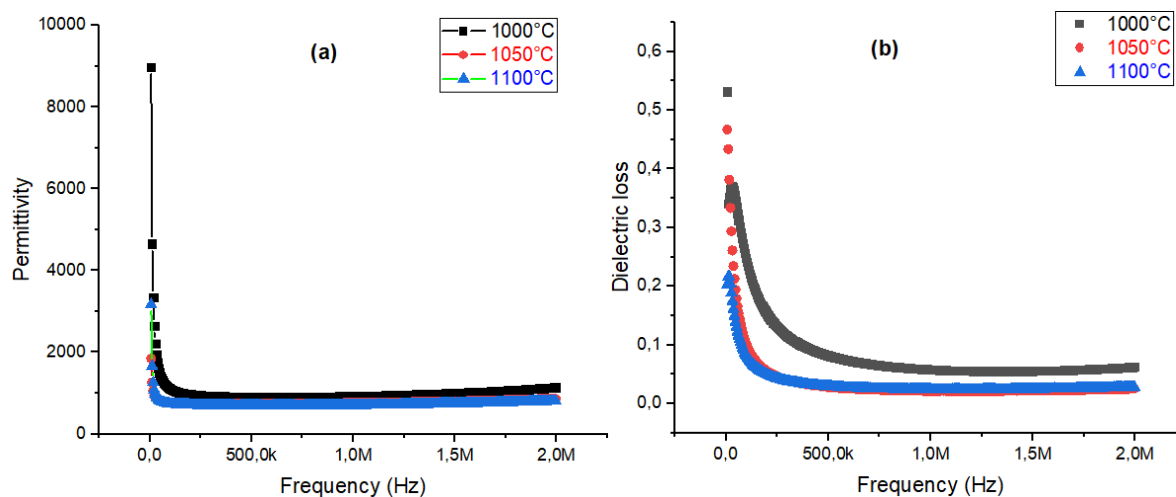
Figure 9. Frequency dependence of permittivity and dielectric loss at temperature 400°C for SrTiO$_3$ ceramics

4. CONCLUSION

The SrTiO$_3$ powders were prepared via the sol-gel method under various calcination temperatures. X-ray diffraction shows that the pure perovskite phase of the ST powders was obtained with calcination condition at 600°C for 6 hours, increase in calcination temperature, lattice parameter and unit cell volume. On the other hand, the average crystallite size increases from 20.74 to 30.53 nm as the calcination temperature increases from 600 to 700°C respectively. The calcination temperature has also a huge influence on the indirect band gap energy. Indeed, strontium titanate has an indirect band gap energy of 1.2eV at 600°C which increases with the increasing of temperature up to 3.32eV at 800°C. Furthermore, obtained results show that the increase in the sintering temperature induces the increase in the grain size. However, study of the dielectric properties, show an interesting stability of the permittivity of sintered ceramics at 1100°C (especially for f > 100 kHz) and that the samples sintered at 1100°C have a smaller (0.021) and stable dielectric losses as a function of frequency, which provide a large scale of several applications fields such as surge protection of electronic devices.

ACKNOWLEDGEMENTS

REFERENCES

[1] J. Gerblinger, K.H. Hardtl, H. Meixner, R. Aigner., A Comprehensive Survey. 8 (199) 181–219

[2] R. Moos, T. Bischoff, W. Menesklou, K.H. Hardtl., J. Mater. Sci. 32 (1997) 4247–4252

[3] S. Steinsvik, R. Bugge, J. Gjonnes, J. Tafto, and T. Norby., J. Phys. Chem. Solids. 58 (6) (1997) 969–976

[4] Y.L. Xu, X.H. Zhou, O. Toft Sørensen., Actuators B. 65 (2000) 2–4

[5] A. A. Adewale , A. Chik, R. M. Zaki, F. C. Pa, Y. C. Keat and N. H. Jamil., International Journal of Nanoelectronics and Materials. 12 (4) (2019) 477-484

[6] A. A. Adewale and A. Chik,, International Journal of Nanoelectronics and Materials. 12 (1) (2019) 11-18

[7] X.H. Zhou, O. T. Sørensen, Y.L. Xu., Actuators B. 41 (1997) 177–182

[8] W. Menesklou, H.-J. Schreiner, K.H. Hardtl, E. Ivers-Tiffee. Actuators B. 59 (1999) 184–189

[9] T. Wang , M. Qiao, Y. Liu , T. Liu , S. Xu., Optics Communications. 474 (2020) 126168

[10] V. Dwij, B. Krishna, S. Tyagi, G. Sharma, V. Sathe., Physica B: Physics of Condensed Matter. 620 (2020) 413265

[11] J. H. Lin, C.S. Hwang, F.R. Sie., Materials Research Bulletin. 122 (2020) 110650

[12] R. Moos, W. Menesklou, H.-J. Schreiner, K.H. Hardtl., Sens. Actuators B. 67, (2000) 178–183

[13] X. Zhou, O. Toft Sørensen, Q. Cao, Y. Xu., Sens Actuators B. 65 (2000) 52–54.

[14] A.J. Feighery, J.C.C. Abrantes, J.A. Labrincha, J.M.F. Ferreira, J.R. Frade, . Actuators B. 75 (2001) 88–94

[15] T. Ding, W. Jia., Actuators. B82 (2002) 284–286

[16] C. Xu, J. Tamaki, N. Miura, N. Yamazor., Actuators B., 3, (1991) 147–155

[17] O.K. Tan, W. Cao, W. Zhu., Actuators B. 63 (1–2) (2000) 129–134

[18] J. Z. Jiang, R. Lin, W. Lin, K. Nielsen, S. Mørup, K. Dam-Johansen, R. Clasen., J. Phys. D: Appl. Phys. 30 (1997) 1459–1467

[19] W. Menesklou, H.-J. Schreiner, K. H. Härdtl, E. Ivers., *Sensors and Actuators B*. **59** (1999) 184-189

[20] R. Meyer, R. Waser., Sensors and Actuators. B101(2004) 335-345

[21] V. A. Purcar, V. Rădiţoiu,A. Dumitru,C.A. Nicolae, A.N. Frone, M. Anastasescu, A. Rădiţoiu, M.F. Raduly,R.A. Gabor,S. Căprărescu., *Appl. Surf. Sci. 487 (*2019) 819–824

[22] C.I. Spataru, V. Purcar, M. Ghiurea, C. Radovici,G. Stanga, D. Donescu,. *J. Sol-Gel Sci. Technol. 65 (*2013) 344–352

[23] L. A. Znaidi, review. *Mater. Sci. Eng. B*. *174* (2010) 18–30

[24] A.E. Danks, S.R.Hall, Z. Schnepp, *Mater. Horizons. 3 (*2016) 91–112

[25] C.-Q. Ye, Intech Open: London, UK, 2018

[26] V. Purcar, R. Şomoghi,S.G. Niţu, C.A. Nicolae,E. Alexandrescu,I.C. Gîfu, A.R. Gabor, H. Stroescu, R. Ianchiş, S. Căprărescu, et al., *Nanomaterials. (*2017) 439

[27] M. Fu.;Y. Li, S. Wu, P. Lu, J. Liu, F. Dong., *Appl. Surf. Sci. 258 (*2011) 1587–1591

[28] A. Elbasset, Lamcharfi, T., Abdi, F., Mrharrab, L. and Sayouri., Indian Journal of Science and Technology. 8(12) (2015) 56348

[29] A Elbasset, S Sayouri, F Abdi, T Lamcharfi and L Mrharrab., XII Maghreb Days of Material Sciences , IOP Conf. Series: Materials Science and Engineering. 186, (2017) 012018

[30] A. Elbasset, S. Sayouri., Adv. Mater. Lett. 6(11) (2015) 999-1003

[31] N. F. Muhamad, R. A. M. Osman, M. S. Idris, M. N. M. Yasin, M. F. Jamlos, N. A. M. Ahmad Hambali and M. N. Derman., International Journal of Nanoelectronics and Materials. 11 (2018) 231-236

[32] Z. Song, H.X. Liu, S.J. Zhang, Z.J. Wang, Y.T. Shi, H. Hao, M.H. Cao, Z.H. Yao, Z.Y. Yu., J. Eur. Ceram. Soc. 34, (2014) 1209-1217

[33] D. T. T. Phuong; N. Xuan Huy, L. T. Mai Oanh, D. D. Bich, T. T. Minh Chau., Communications In Physics. 27, No. 2 (2017) 173-179

[34] T. Ostapchuk, J. Petzelt, V. Železný, A. Pashkin, J. Pokorný, I. Drbohlav, R. Kužel, D. Rafaja, B. P. Gorshunov, M. Dressel, Ch. Ohly, S. Hoffmann-Eifert, and R. Waser., phys review B66, (2002) 235406

[35] D. J. Kok, K. Irmscher, M. Naumann, C. Guguschev, Z. Galazka, R. Uecker., Status Solidi A. 212, 9, (2015) 1880–1887

[36] T. Bieger, J. Maier, and R.Waser., Solid State Ion. 53–56, 1992) 578

[37] J.C. Sczancoski, L.S. Cavalcante, T. Badapanda, S.K. Rout, S. Panigrahi, V. R. Mastelaro, J.A. Varela, M.S. Li, E. Longo., Solid State. Sci. 12, (2010) 1160–1167

[38] E.A.V. Ferri, J.C. Sczancoski, L.S. Cavalcante, E.C. Paris, J.W.M. Espinosa, A.T. de Figueiredo, P.S. Pizani, V.R. Mastelaro, J.A. Varela, E. Longo., Mater. Chem. Phys. 117, (2009) 192–198

[39] P.K. Sharma, G. L. Messing, D. K. Agarwal., Thin solid films. 491 (2005) 204–211

[40] Z. Wang, M. Cao, Z. Yao, Q. Zhang, Z. Song, W. Hu, Q. Xu, H. Hao, H. Liu, Z. Yu., Journal of the European Ceramic Society. 34 (2014) 1755–1760